Available online at www.sciencedirect.com
SCIENCE DIRECT®
ELSEVIER
Composite Structures 69 (2005) 322–328
COMPOSITE STRUCTURES
www.elsevier.com/locate/compstruct

Evaluation of equivalent stiffness properties of corrugated board

M.E. Biancolini *

Department of Mechanical Engineering, University of "Tor Vergata", Via del Politecnico 1, 00133 Rome, Italy

Available online 13 September 2004

Abstract

A numerical approach to evaluate the stiffness parameters for corrugated board is presented in this paper. The method is based on a detailed micromechanical representation of a region of corrugated board modelled by means of finite elements.

In order to define the stiffness properties, energy equivalency is imposed between the discrete model and the equivalent plate. Exploiting a transformation matrix capable to map a constant strain/curvature vector for the equivalent plate in a displacement field of the FEM boundary nodes, it is possible to express an equivalent ABD matrix as a function of the boundary condensed stiffness matrix of the FEM model.

Practical examples dealing with the computation of stiffness properties of paperboard are presented.

Keywords: Corrugated board; Homogenisation; Plate stiffness properties

1. Introduction

Corrugated board is widely used in the packaging industry. The main advantages are lightness, recyclability and low cost. This makes the material the best choice to produce containers devoted to the shipping of goods.

Furthermore, examples of structure design based on corrugated boards can be found in different fields. The design of a complete structure was presented by El Damatty et al. [1] which proposed a calculation methodology for a cardboard shelter and by Ahmed et al. [2] which presented a study about the design of a corrugated roof built with steel and paperboard.

Structural analysis of paperboard components is a crucial topic in the design of containers. It is required to investigate their strength properties because they have to protect the goods contained from lateral crushing and compression loads due to stacking.

In fact for this load condition, buckling may occur. Its avoidance requires a deep knowledge of stiffness properties of paperboard.

In the reviewed literature a study about the strength of paperboard can be found, including the effect of local buckling exhibited by the liners [3]. However, in such study elastic properties are evaluated by means of the Composite Laminate Plate Theory. A numerical procedure was proposed by Urbanik and co-workers [4,5] to evaluate global and local instability of paperboard sheets loaded both in machine direction and cross direction, taking into account the actual microstructure with a simplified tooth shaped geometric model.

Experimental evaluation of transverse shear stiffness and bending stiffness was presented in [6]. Recently an extension of Classical Laminated Plate Theory that considers averaged fluting property was presented [7].

In this work, a numerical procedure for the evaluation of equivalent stiffness properties of corrugated board is proposed. The method is based on a discrete modelling of the local geometry of corrugated board by means of a finite elements model that was proven to be effective in a work previously presented [8]. Orthotropic shell elements are used to reproduce the actual behaviour of paper.

Equivalent elastic properties of the assembled structure are determined with an homogenisation procedure

* Fax: +39 06 202 1351.
E-mail address: biancolini@ing.uniroma2.it

0263-8223/$ - see front matter © 2004 Elsevier Ltd. All rights reserved.
doi:10.1016/j.compstruct.2004.07.014

Notation

κ	strain/curvature vector
$[\mathbf{K}]$	boundary stiffness matrix
$[\mathbf{A}_e]$	displacement field transformation matrix
E_L	Young modulus of paper in machine direction
E_T	Young modulus of paper in cross direction
G_{LT}	shear modulus of paper
ν_{LT}	Poisson modulus of paper
t	paper sheet thickness
h	paperboard sheet thickness
L	fluting projected length
l	fluting actual length
Ψ	l/L corrugation ratio

able to extract an equivalent element "corrugated board" that exhibits the same behaviour of a detailed model. In technical literature the equivalent element is approximated invoking the classical laminate theory, i.e. assuming that the corrugated medium is represented by an equivalent orthotropic lamina. However this approach neglects to consider that for a corrugated sheet equivalent lamina flexural and extensional material differs [9] and that the connections between corrugation and liners are limited to the glued regions [10].

Among commercial FEM codes suitable to study the problem, in this work MSC/Nastran implementation was adopted. The equivalent composite matrix is computed by a pre-processing stage in which the material properties are integrated through the thickness and then used as an input data for a shell element that handles different materials for flexure, extension, flexure–extension coupling and transverse shear. Adopting the proposed procedure, this pre-processing stage is replaced by the homogenisation stage and the resulting matrix are input directly in the shell property.

The homogenisation of the micromechanical model is executed performing a static condensation, leaving in the analysis set only the degree of freedom of the boundary nodes, and obtaining an equation between the equivalent stiffness matrix and the reduced FEM matrix through an energetic approach, simply defining a transformation able to map a state of pure strain/curvature of the plate (defined in a six dimension space) in a displacement fields of the boundary nodes (defined in a $5 * n$ dimension space, where n is the number of the boundary nodes accounting five dofs for node).

The fully automated procedure is first validated with simple application for which a closed form solution is available, and then exploited to perform a parametric analysis for different paperboards.

2. Geometry of the investigated structure

In this work a simple shape of corrugated board, consisting of a corrugated core (*fluting*), enclosed between two flat faces (*liners*), is investigated. In Fig. 1, a sketch

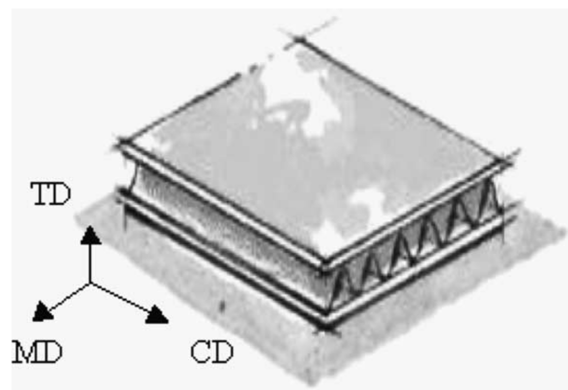

Fig. 1. Corrugated board geometry and principal material directions.

of an actual region of corrugated board is represented. Corrugated board has directional properties for the anisotropy of building paper and for the corrugated structure of the core. Symmetry directions are defined according to the notation adopted for the paper: the machine direction (MD) corresponds to the winding direction of the spindle, the cross direction (CD) corresponds to direction transversal to MD in the sheet plane, and the thickness direction (TD) corresponds to the direction along the thickness out of the sheet plane. Being the corrugated board manufactured in a continuum process, the fluting is corrugated travelling along the machine direction. Resulting structure stiffness is then a trade off between paper anisotropy and geometrical anisotropy, because papers fibres are preferably oriented in machine direction, leading to an higher modulus in this direction while fluting geometry produces higher cross section area and moment of inertia in the cross direction.

In order to correctly reproduce the global stiffness, material moduli (E_L, E_T, ν_{LT}, G) of each layer are required, together with the geometrical parameters that are the thickness of each layer (t), the corrugation height (h) and length (H), and the actual corrugation shape. A geometric parameter widely used for corrugated structures is the corrugation ratio (ψ) between the actual length of a corrugation and the projected length.

3. Evaluation of stiffness properties

As exposed in Section 1, the main goal of this work is to obtain the stiffness properties of a region of corrugated board useful to analyse the region by means of an equivalent lamina. According to the Classical Laminates Plate Theory (CLPT) the investigated structure may be represented as a three plies laminate. It is assumed that the corrugated core behaves as a single homogenous lamina. However, due to the corrugated structure, the core cannot be reduced to an equivalent orthotropic material valid for both bending and stretching. Furthermore, the connection between the core and the facing is not continuous but confined to the crests. For these reasons was chosen to extract equivalent stiffness from a full detailed FEM model of a portion of corrugated board.

The energetic approach proposed in [11], in which a region of fibrous material was reduced to an equivalent anisotropic homogenous material, was herein followed.

The homogenisation procedure devised is general and can be applied to extract the equivalent lamina for an arbitrary region modelled with finite elements. In Fig. 2(a) the FEM model for corrugated board local geometry is represented.

The first step of the homogenisation procedure consists of a static condensation, in which the internal nodes (i) are removed leaving only the external nodes (e). As depicted in Fig. 2(b), external nodes are all the nodes at the boundary of the FEM model representing the edges of the equivalent lamina.

Nodal loads at the boundary can be evaluated from nodal displacements at boundary by means of the condensed stiffness matrix, valid for zero load at internal nodes:

$$[\overline{\mathbf{K}}] \cdot \{u_e\} = \{F_e\}, \tag{1}$$

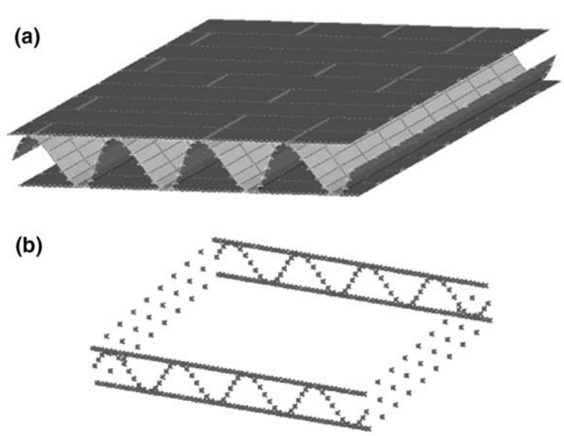

Fig. 2. FEM model of microgeometry (a) and boundary nodes (b).

being

$$[\overline{\mathbf{K}}] = [\mathbf{K}_{ee}] - [\mathbf{K}_{ei}] \cdot [\mathbf{K}_{ii}]^{-1} \cdot [\mathbf{K}_{ie}], \tag{2}$$

where overall stiffness matrix was partitioned in four submatrixes as follow:

$$\begin{bmatrix} \mathbf{K}_{ee} & \mathbf{K}_{ei} \\ \mathbf{K}_{ie} & \mathbf{K}_{ii} \end{bmatrix} \cdot \begin{Bmatrix} u_e \\ u_i \end{Bmatrix} = \begin{Bmatrix} F_e \\ 0 \end{Bmatrix}. \tag{3}$$

Assuming a given displacements vector $\{u_e\}$, the total elastic energy stored in the volume is equal to

$$E = \tfrac{1}{2} \cdot \{u_e\}^T \cdot \{F_e\}. \tag{4}$$

In order to establish an energetic equivalence between the FEM modelled region and the equivalent plate, a displacement field needs to be defined. The generalised displacement of each node at the boundary can be directly related to the generalised strain vector of the plate by means of a transformation matrix ($5 \cdot N$ rows, 6 columns).

A strain field according to Kirchoff Love assumption was considered:

$$\begin{pmatrix} \varepsilon_x \\ \varepsilon_y \\ \gamma_{xy} \end{pmatrix} = \begin{pmatrix} \varepsilon_x^0 \\ \varepsilon_y^0 \\ \gamma_{xy}^0 \end{pmatrix} + z \begin{pmatrix} \kappa_x \\ \kappa_y \\ \kappa_{xy} \end{pmatrix} = \begin{pmatrix} \frac{\partial u}{\partial x} \\ \frac{\partial v}{\partial y} \\ \frac{\partial v}{\partial x} + \frac{\partial u}{\partial y} \end{pmatrix}, \tag{5}$$

that permit to calculate by integration the in plane displacement field as follows:

$$\begin{aligned} u(x,y,z) &= \frac{y}{2}\gamma_{xy}^0 + \frac{yz}{2}\kappa_{xy} + \varepsilon_x^0 x + xz\kappa_x, \\ v(x,y,z) &= \frac{x}{2}\gamma_{xy}^0 + \frac{xz}{2}\kappa_{xy} + \varepsilon_y^0 y + yz\kappa_y. \end{aligned} \tag{6}$$

Recalling the definition of curvatures,

$$\begin{pmatrix} \kappa_x \\ \kappa_y \\ \kappa_{xy} \end{pmatrix} = \begin{pmatrix} -\frac{\partial^2 w}{\partial x^2} \\ -\frac{\partial^2 w}{\partial y^2} \\ -\frac{\partial^2 w}{\partial x \partial y} \end{pmatrix}, \tag{7}$$

and after a first integration, the field of angular rotation is obtained:

$$\begin{aligned} \phi_y(x,y) &= -\frac{\partial w}{\partial x} = x\kappa_x + \frac{y}{2}\kappa_{xy}, \\ \phi_x(x,y) &= \frac{\partial w}{\partial y} = -y\kappa_y - \frac{x}{2}\kappa_{xy}. \end{aligned} \tag{8}$$

After a further integration the vertical displacement field results as:

$$w(x,y) = -\frac{x^2}{2}\kappa_x - \frac{xy}{2}\kappa_{xy} - \frac{y^2}{2}\kappa_y. \tag{9}$$

Considering the position of the nodes at the boundary and the constant generalised strain vector, the displacement of each node can be expressed by means of the following transform:

$$\begin{pmatrix} \vdots \\ \begin{pmatrix} u_x \\ u_y \\ u_z \\ \phi_x \\ \phi_y \end{pmatrix}_j \\ \vdots \end{pmatrix} = \begin{bmatrix} \vdots \\ [\mathbf{A}_e]_j \\ \vdots \end{bmatrix} \cdot \begin{pmatrix} \varepsilon_x^0 \\ \varepsilon_y^0 \\ \gamma_{xy}^0 \\ \kappa_x \\ \kappa_y \\ \kappa_{xy} \end{pmatrix}, \tag{10}$$

written in compact form as

$$\{u\}^{\mathrm{T}} = [\mathbf{A}_e] \cdot \{\kappa\}, \tag{11}$$

where the generic submatrix, related to a single node j located at (x^j, y^j, z^j) is:

$$[\mathbf{A}_e]_j = \begin{bmatrix} x^j & 0 & \frac{y^j}{2} & x^j z^j & 0 & \frac{y^j z^j}{2} \\ 0 & y^j & \frac{x^j}{2} & 0 & y^j z^j & \frac{x^j z^j}{2} \\ 0 & 0 & 0 & -\frac{x^j x^j}{2} & -\frac{y^j y^j}{2} & -\frac{x^j y^j}{2} \\ 0 & 0 & 0 & 0 & -y^j & -\frac{x^j}{2} \\ 0 & 0 & 0 & x^j & 0 & \frac{y^j}{2} \end{bmatrix}. \tag{12}$$

Recalling the definition of the strain energy for the discrete model:

$$\begin{aligned} E &= \tfrac{1}{2} \cdot \{u_e\}^{\mathrm{T}} \cdot [\overline{\mathbf{K}}] \cdot \{u_e\} \\ &= \tfrac{1}{2} \cdot \{\kappa\}^{\mathrm{T}} \cdot [\mathbf{A}_e]^{\mathrm{T}} \cdot [\overline{\mathbf{K}}] \cdot [\mathbf{A}_e] \cdot \{\kappa\}, \end{aligned} \tag{13}$$

and considering that for a shell subjected to bending and traction the internal strain energy is:

$$E = \tfrac{1}{2} \cdot \{\kappa\}^{\mathrm{T}} \cdot [\mathrm{ABD}] \cdot \{\kappa\} \cdot \{\mathrm{area}\}, \tag{14}$$

overall stiffness matrix for the laminate could be easily extracted form the discrete stiffness matrix as

$$[\mathrm{ABD}] = \frac{[\mathbf{A}_e]^{\mathrm{T}} \cdot [\overline{\mathbf{K}}] \cdot [\mathbf{A}_e]}{\{\mathrm{area}\}}. \tag{15}$$

4. Homogenisation procedure validation

The proposed numerical method was validated performing a direct comparison between predicted results and theoretical or literature solutions. Two simple case were tested: the first consists in the modelling of a single orthotropic lamina, with an offset respect to the reduction plane, the second is the study of a sandwich reported in [12].

As far as the single lamina is concerned, ABD matrix was extracted for a square region of paperboard KL5 (see Table 3 for details about this material), obtaining the following ABD matrix, where values lower than 10^{-10} where truncated at zero:

$$\mathrm{ABD}_n = \begin{pmatrix} 1.024\times10^6 & 1.747\times10^5 & 0 & 1792.71 & 305.702 & 0 \\ 1.747\times10^5 & 5.206\times10^5 & 0 & 305.704 & 909.796 & 0 \\ 0 & 0 & 2.496\times10^5 & 0 & 0 & 436.402 \\ 1792.71 & 305.704 & 0 & 3.145 & 0.536 & 0 \\ 305.702 & 909.796 & 0 & 0.536 & 1.597 & 0 \\ 0 & 0 & 436.402 & 0 & 0 & 0.766 \end{pmatrix}.$$

Table 1
Validation results

		Corrugated structure			Isolated lamina		
		Buannic	Model	Diff. %	CLPT	Model	Diff. %
A_{11}	Pa m	1.11E+09	1.11E+09	0.54	1.02E+06	1.02E+06	0.10
A_{22}	Pa m	1.36E+09	1.38E+09	1.47	5.21E+05	5.21E+05	−0.12
A_{12}	Pa m	3.32E+08	3.41E+08	2.47	1.75E+05	1.75E+05	−0.23
A_{33}	Pa m	4.12E+08	4.11E+08	−0.27	2.49E+05	2.50E+05	0.08
D_{11}	Pa m^3	9.20E+05	9.20E+05	0.08	3.141	3.145	0.13
D_{22}	Pa m^3	9.82E+05	9.93E+05	1.08	1.6	1.597	−0.19
D_{12}	Pa m^3	2.76E+05	2.77E+05	0.47	0.538	0.536	−0.37
D_{33}	Pa m^3	3.22E+05	3.27E+05	1.58	0.766	0.766	0.00
B_{11}	Pa m^2				1790.924	1792.71	0.10
B_{22}	Pa m^2				912.154	909.796	−0.26
B_{12}	Pa m^2				306.484	305.704	−0.25
B_{33}	Pa m^2				436.516	436.402	−0.03

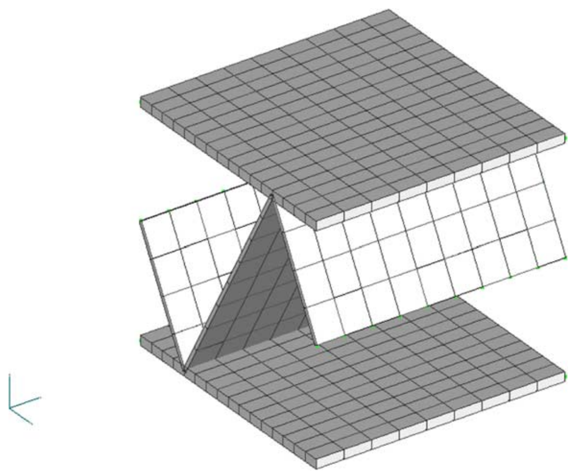

Fig. 3. FEM model of literature corrugated structure T2.

It's interesting to notice that the full matrix is computed by the code obtaining a perfect symmetry.

Theoretical values for the same problem are easily calculated according to the lamination theory.

Comparison between the theoretical and numerical results is summarised in Table 1 where the maximum difference observed is about 0.4%.

The second test concerns with an assembled sandwich structure consisting of a tooth shaped corrugated core enclosed between two sheets. A reference solution is available from Buannic et al. [12]. According to literature notation the panel T2 was investigated. The FEM model used with the present method for the sandwich T2 is reported in Fig. 3. Error estimation was performed as for the first test obtaining a maximum deviation lower than 2.5%.

5. Results and discussion

The proposed model was used to investigate the effect of composition, shape and thickness for a typical corrugated board designed as KLSKL595C, widely employed to build containers that have to withstand with compression loads.

According to GIFCO (*Gruppo Italiano Fabbricanti Cartone Ondulato* the Italian Association of Corrugated Board Manufacturers) the acronym KLSKL595C refers to a single wall corrugated board built with a liner of KL5, a fluting of S9 with a "C" corrugation and a liner of KL5. Typical values for the geometric parameters are reported in Table 2; building paper mechanical properties are summarised in Table 3.

Table 2
"C" corrugation shape parameters

H	Paperboard sheet thickness	3.5–4.4
L	Fluting projected length	7.3–8.1
Ψ	l/L corrugation ratio	1.41–1.45

A corrugated board 3.8 mm thick with 8 mm fluting projected length was chosen as reference material. Corrugation ratio is 1.435 as results from an actual section that was used also to record the wave shape.

Several parameters were then perturbed to quantify the effect on panel stiffness.

As depicted in Figs. 4–6 the original shape (Fig. 4) was varied adopting a saw-tooth profile (Fig. 5), and a sinusoidal profile (Fig. 6), but keeping the same thickness and the same projected length.

Also the thickness was varied considering a reduced value (3.5 mm) and an enlarged value (4.1 mm), but keeping constant the projected length and the adimensional profile function.

The last analysis executed concerns with the building material used for fluting and liners, i.e. considering a worst fluting (KLSKL565C), a worst liner (TST595C), the combined effect (TST565C) and a better liner material (KLSKL696C).

Investigated parameters, with the obvious exception of fluting shape, can be directly controlled by the manufacturer in order to obtain the best performance of the corrugated board. This goal can be achieved acting on paper composition, and in some extent controlling corrugated board thickness with a proper adjustment of the corrugator working parameters. The last adjustment has to be scheduled, together with corrugator cylinders periodic substitution, in order to compensate fluting height reduction that results from corrugating cylinders wearing.

The computed results are reported in Table 4. Both in plane and out of plane stiffness matrix non-null components are summarized collecting by columns the parameters resulting for each configuration investigated. In the

Table 3
Corrugated board paper parameters

Name	E_L (MPa)	E_T (MPa)	G_{LT} (MPa)	ν_{LT}	ρ (g/m^2)	t (mm)
S-6	3226	1610	825	0.34	150	0.25
S-9	2614	1532	724	0.32	175	0.30
KL-3	3940	1656	925	0.37	150	0.20
KL-5	3326	1694	859	0.34	200	0.29
KL-6	3292	1853	894	0.32	230	0.32
T-5	2500	1256	641	0.34	185	0.29

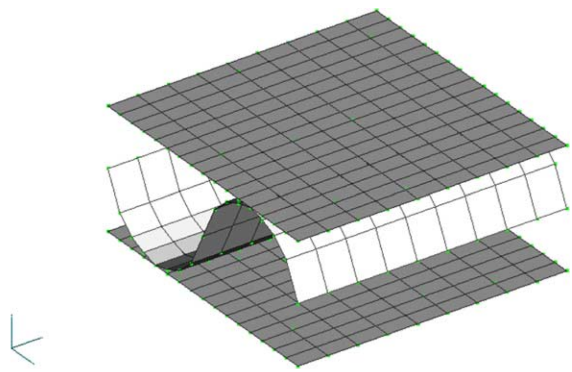

Fig. 4. Corrugated board actual profile FEM model.

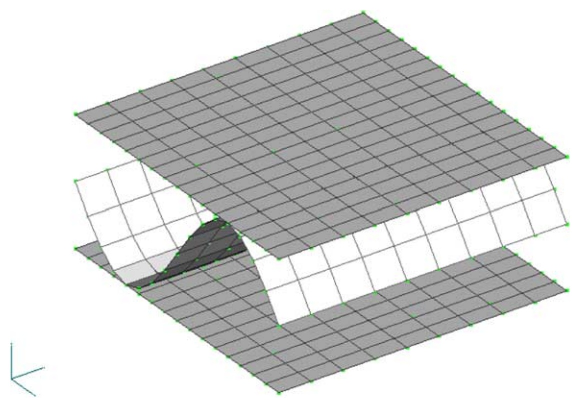

Fig. 5. Sine profile FEM model.

next to last row mean geometric value between flexural stiffness in MD and CD is reported. This parameter is proportional to buckling load of a simple supported panel, as reported in [13], and gives a good index of box compression strength. Relative variation of such parameter with respect to the base material of the first column is also reported in the last row of the table.

The first corrugated board parameter investigated is the shape and obtained results shows slight variations in stiffness parameters. This is mainly due to the higher contribution of the liners. Although the original shape seems to be the best for flexural stiffness, the loss in mean flexural stiffness observed for other shapes (4.4% adopting a saw tooth profile, 1.66% adopting a sine profile) is related also to a reduction of corrugation ratio, because the projected length was considered fixed to the reference value. This means that the reduction in performances is partially compensated by a reduction in cost.

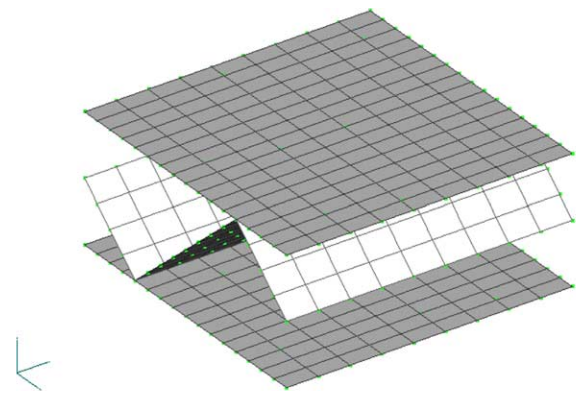

Fig. 6. Sawtooth profile FEM model.

Some variations could be appreciated changing fluting composition. In fact the replacing of S9 with a worse material S6 produces a lost of about 7% (−7.1% between KLSKL595 and KLSKL565, −7.47% between TST595 and TST565).

A strong variation is observed varying liners composition with a great stiffness loss (KLSKL595/TST595 −21.9%) or gain (KLSKL595/KLSKL696 +16.53%) leaving the same fluting material.

The importance of liners is also remarked by the effect of global thickness. A 0.3 mm thickness increment (3.8 mm/4.1 mm +18%) produces about the same effect of changing liners composition (KL5/KL6 16.5%). The same trend is observed comparing a thickness reduction

Table 4
Parametric analysis results

Parameter	Unit									
Thickness	mm	3.8	3.8	3.8	3.8	3.8	3.8	3.8	3.5	4.1
Shape		Base	Saw tooth	Sine	Base	Base	Base	Base	Base	Base
Composition		KLSKL595	KLSKL596	KLSKL597	KLSKL565	TST565	TST595	KLSKL696	KLSKL595	KLSKL595
A_{11}	Pa m	2,124,000	2,158,000	2,130,000	2,119,000	1,608,000	1,613,000	2,314,000	2,131,000	2,118,000
A_{22}	Pa m	1,696,000	1,660,000	1,676,000	1,607,000	1,344,000	1,433,000	1,920,000	1,671,000	1,722,000
A_{12}	Pa m	368,300	379,900	371,700	365,300	280,800	283,600	426,100	369,600	367,300
A_{33}	Pa m	671,400	677,600	674,000	650,100	523,100	544,300	743,600	677,300	665,900
D_{11}	Pa m^3	6.438	6.37	6.408	6.069	4.593	4.874	7.266	5.393	7.577
D_{22}	Pa m^3	4.143	3.824	4.025	3.793	3.03	3.335	4.985	3.449	4.905
D_{12}	Pa m^3	1.103	1.092	1.099	1.037	0.793	0.845	1.324	0.924	1.298
D_{33}	Pa m^3	1.779	1.655	1.73	1.648	1.28	1.388	2.074	1.49	2.093
$\sqrt{D_{11} \cdot D_{22}}$	Pa m^3	5.165	4.935	5.079	4.798	3.731	4.032	6.018	4.313	6.096
$\Delta\sqrt{D_{11} \cdot D_{22}}$	%	0.00	−4.44	−1.66	−7.10	−27.77	−21.93	16.53	−16.49	18.04

(3.8 mm/3.5 mm −16.5%) with a change of liners (KL5/T5 −22%).

6. Conclusions

In this paper a numerical procedure suitable for corrugated board panel stiffness estimation was presented. A local model representing the actual microgeometry was adapted to extract ABD matrix using a homogenisation procedure. The reliability of the method was checked with a series of numerical test obtaining accurate results.

Proposed model was then used to perform a parametric investigation about influence of local parameter in corrugated board panel stiffness.

In order to show how material stiffness is related to final product performance, the mean geometric value between flexural stiffness in MD and CD was calculated. This parameter is proportional to buckling load of a simple supported panel.

With respect to the base material KLSKL595 the worst reduction in mean geometric flexural stiffness obtained was −27.7% for TST565 while the best performances was exhibited by KLSKL595 4.1 mm thick with an increment of 18.04%. Absolute range was found equal to [3.731 $\mathrm{Pa\,m^3}$, 6.096 $\mathrm{Pa\,m^3}$].

Overall results permit to conclude that stiffness parameters are weakly controlled acting on fluting shape and composition because the main contribution is provided by the liners that stiffen the material with their composition and their distance from midplane.

References

[1] El Damatty AA, Mikhail A, Awad AA. Finite element modeling and analysis of a cardboard shelter. Thin-Walled Struct 2000;38:145–65.

[2] Ahmed E, Wan Badaruzzaman WH, Wright HD. Experimental and finite element study of profiled steel sheet dry board folded plate structures. Thin-Walled Struct 2000;38:125–43.

[3] Nyman U, Gustafsson PJ. Material and structural failure criterion of corrugated board facings. Compos Struct 2000;50:79–83.

[4] Urbanik TJ. Machine direction strength theory of corrugated fiberboard. J Compos Technol Res 1996;18(2):80–8.

[5] Johnson Jr MW, Urbanik TJ. Analysis of the localized buckling in composite plate structures with application to determining the strength of corrugated fiberboard. J Compos Technol Res 1989;11(4):121–7.

[6] Nordstrand T, Carlsson LA. Evaluation of transverse shear stiffness of structural core sandwich plates. Compos Struct 1997;37:145–53.

[7] Aboura Z, Talbi N, Allaoui S, Benzeggagh ML. Elastic behaviour of corrugated cardboard: experiments and modeling. Compos Struct 2004;63:53–62.

[8] Biancolini ME, Brutti C. Numerical and experimental investigation of the strength of corrugated board packages. Packag Technol Sci 2003;16(2):47–60.

[9] Briassoulis D. Equivalent orthotropic properties of corrugated sheets. Comput Struct 1996;23(2):129–38.

[10] Bryan ER, El Dakhakhni WM. Shear flexibility and strength of corrugated decks. J Struct Div ASCE 1968;94(ST 11):2549–80.

[11] Stahl DC. A three dimensional network model for a low density fibrous composite. J Eng Mater Technol 1998;120(2):126–30.

[12] Buannic N, Cartraud P, Quesnel T. Homogenization of corrugated core sandwich panels. Compos Struct 2003;59:299–312.

[13] McKee C, Gander JW, Wachuta JR. Compression strength formula for corrugated boxes. Paperboard Packag 1963;23:149–59.